Nonlinear optimal control of epidemic dynamics under healthcare capacity constraints

Original Article

Abstract

Healthcare saturation can amplify epidemic mortality, yet most models assume constant fatality rates. This study develops a nonlinear optimal control framework for an SUDTHREV epidemiological model incorporating healthcare-capacity-dependent mortality via a sigmoidal function. The Pontryagin Maximum Principle is used to solve the optimal control problem, resulting in a coupled forward-backward system for vaccination, testing, treatment, and transmission techniques. Numerical findings indicate a shift to a subcritical regime with a 90% decrease in mortality and an 85% decrease in peak infections. Sensitivity analysis shows that survival outcomes are influenced by therapy, but epidemic magnitude is determined by transmission controls. These findings provide a framework for designing interventions in capacity-constrained settings.

Keywords: Healthcare saturation; Optimal control theory; Sigmoidal response; Pontryagin Maximum Principle

1 Introduction

Infectious disease outbreaks continue to pose significant challenges to public health systems, especially in low- and lower-middle-income countries (LLMICs), where only about 22% of health facilities meet pandemic capacity standards and demand surges frequently exceed capacity (Madhav et al., 2017; Omosigho et al., 2023; Falodun et al., 2025; Hakim and Haque, 2026). Emerging pathogens (such as COVID-19, Cholera, mpox) and re-emerging diseases (such as tuberculosis and measles) test weak infrastructures, resulting in high mortality and significant social and economic disruption (Okeke et al., 2022; Kaba et al., 2025).

A structured framework for studying the spread of infectious diseases and assessing intervention strategies has long been offered by mathematical models (Kretzschmar and Wallinga, 2009; Durojaye

and Odeyemi, 2019; Durojaye et al., 2019; Odeyemi et al., 2023; Okafor et al., 2025; Pathak and Kota, 2025). Classical compartmental models, including extensions with optimal control, have been extensively used to investigate the effects of transmission reduction, testing, treatment, and vaccination on epidemic dynamics (Tolles and Luong, 2020; Khan et al., 2022). These approaches have resulted in significant discoveries with regard to the cost-effectiveness of the intervention strategies and the threshold requirements for disease elimination (Shretta et al., 2017; Biswas et al., 2017; Kuddus et al., 2024; Olaiju et al., 2025a; Antony Oliver et al., 2025).

In spite of these advances, one important drawback remains evident in the majority of the literature. In the context of the epidemiological models, including the SIR, SIRD, and SEIR models, the mortality rates remain constant or linearly dependent. This reveals the implicit assumption that the healthcare facilities operate under stable conditions. However, this overlooks the fact that the mortality rates can increase in scenarios where the healthcare facilities are overwhelmed by the high epidemic intensity. Empirical evidence collected from the recent epidemic scenarios shows that the healthcare facilities considerably affect the mortality rates, with the rates increasing with the demand for hospitalizations reaching the capacity limits (Tolles and Luong, 2020; Martin et al., 2021; Xue et al., 2025). This suggests the presence of a non-linear feedback relationship, which is not adequately addressed by the standard models, including the interactions between the healthcare burdens and the disease progression.

A number of modelling studies have attempted to incorporate constraints on healthcare capacities, such as those discussed in (Marshall et al., 2015; Vugrin et al., 2015; Singla, 2020; Shahverdi et al., 2023; Petanidis et al., 2025). However, such implementations are often modelled using simple or discontinuous structures that do not accurately reflect continuous transitions from managed to overwhelmed states. In addition, the relationship between capacity-dependent mortality and optimal intervention methods has not been sufficiently explored. In particular, current optimal control models devote little attention to understanding how nonlinear mortality affects optimal intervention strategies, typically focusing on minimising infection prevalence or intervention cost, as discussed in (Xia et al., 2024; Idisi et al., 2025; Liu et al., 2025; Nainggolan et al., 2025; Caravaggio et al., 2026). In contrast, linear models fail to account for excess mortality resulting from high infection prevalence, leading to a saturation of healthcare capacities, a problem that can be reduced using nonlinear models. Thus, current models may not fully appreciate the need to prevent such saturation and fail to understand trade-offs, as discussed in (Yadav and Akhter, 2021; Thokala et al., 2025; Hakim and Haque, 2026; Kowalewska et al., 2026).

Furthermore, current optimal control models do not reliably predict staged disease progression, as discussed in (Kretzschmar et al., 2022). The relationship between undetected infections, detected cases, treatments, hospitalisations, and mortality is often oversimplified, making it difficult to understand how interventions affect patient outcomes and transmission, as discussed in (Grassly and Fraser, 2008; Qu et al., 2021; Sanz-Lorenzo and Bravo de la Parra, 2024). This oversimplification fails to allow current models to differentiate between controls that reduce transmission and those that affect disease severity and survival.

A nonlinear optimal control model, along with a structured SUDTHREV epidemiological model, will be developed to address these issues, allowing for a more accurate representation of transmission, disease progression, and mortality, dependent on healthcare capacities. A sigmoidal form of a hospital-induced mortality function will be a key part of the model, allowing for a continuous representation of how fatality risk increases with hospitalisation. This formulation allows the model to capture the nonlinear transition from baseline mortality to elevated risk during saturation, connecting epidemic dynamics to healthcare system constraints.

Accordingly, in this framework, a multi-control optimization problem is posed in order to assess different intervention strategies in terms of vaccination, improvement of treatments, increase of testing, and reduction of transmission. The Pontryagin Maximum Principle is applied to the system, yielding a forward-backward formulation for the optimal policies. The trade-off between health effects and resource allocation is made possible by the cost functional.

The objective of this study is to identify how intervention strategies can be most effectively designed to control the spread of the disease while avoiding system overload, hence controlling both the level of infection and mortality rates. By specifically incorporating nonlinear mortality dynamics, this analysis helps clarify how intervention strategies control not just the scale of the epidemic, but its severity as well. This helps to overcome a major drawback of current models by specifically relating optimal control to healthcare-based nonlinear feedback, and hence establishes a basis for understanding the management of epidemics in terms of controlling system behavior in the face of system saturation.

2 Methodology

2.1 Model Structure and Governing Dynamics

We formulate a compartmental epidemiological system that captures disease transmission, clinical progression, healthcare burden, and intervention strategies through a coupled system of nonlinear ordinary differential equations. The total population is partitioned into eight epidemiological states representing susceptible, undetected infected, diagnosed, treated, hospitalized, recovered, disease induced deaths (disease-induced mortality), and vaccinated individuals.

We consider a deterministic compartmental model consisting of eight epidemiological states: susceptible (S), unreported infected (U), detected cases (D), treated individuals (T), hospitalized individuals (H), recovered (R), disease induced deaths (E), and vaccinated (V). The total population evolves under the influence of four time-dependent control variables representing intervention strategies.

The controlled system is given by:

$$\begin{cases} \dot{S} = -\beta(1 - w_1(t))S(U + \rho D) - \xi w_4(t)S + \eta V, \\ \dot{U} = \beta(1 - w_1(t))S(U + \rho D) - (\gamma + \delta w_2(t) + \sigma_u)\, U, \\ \dot{D} = \delta w_2(t)U - (\sigma_d + \phi_d)D, \\ \dot{T} = \sigma_u U + \sigma_d D - (\phi_t + \mu_t)T, \\ \dot{H} = \phi_d D + \phi_t T - (\theta w_3(t) + \bar{\mu}_h(Q))\, H, \\ \dot{R} = \theta w_3(t)H + \gamma U, \\ \dot{E} = \mu_t T + \bar{\mu}_h(Q)H, \\ \dot{V} = \xi w_4(t)S - \eta V. \end{cases} \tag{2.1}$$

where the control variables w_1, w_2, w_3, w_4 represent time-dependent intervention policies associated with transmission mitigation, testing intensification, therapeutic enhancement, and vaccination deployment, respectively (see Table 1). In addition, $\rho \in [0, 1]$ represents the relative infectivity of detected individuals compared to undetected infections, reflecting behavioural changes such as isolation following detection. To capture healthcare system saturation, the hospital-induced mortality rate is modeled as a nonlinear sigmoidal function:

$$\bar{\mu}_h(Q) = \mu_h + \frac{\mu_h^{\max} - \mu_h}{1 + e^{-k(Q - Q_{\text{crit}})}}, \tag{2.2}$$

where Q denotes the hospital burden, approximated by the hospitalized population H. This formulation ensures a smooth transition from baseline mortality to elevated mortality when healthcare capacity is exceeded. The model guarantees non-negativity of solutions and incorporates nonlinear feedback between disease dynamics and healthcare capacity, making it suitable for optimal control analysis under resource constraints.

The model parameters were selected to reflect realistic epidemiological and intervention dynamics. Transmission, detection, treatment, and vaccination processes are governed by parameters summarized in Table 2. The nonlinear hospital-induced mortality function incorporates capacity-dependent effects through a sigmoidal formulation.

Table 1: Control Variables

Control	Description
$w_1(t)$	Transmission mitigation (e.g., distancing, masking)
$w_2(t)$	Testing and detection effort
$w_3(t)$	Treatment and therapeutic intervention
$w_4(t)$	Vaccination deployment

Table 2: Model Parameters

Parameter	**Description**	**Value**
β	Transmission rate	0.8
γ	Recovery rate from unreported infections	0.2
δ	Detection (testing) rate	0.1
σ_u	Progression rate from unreported to treatment	0.05
σ_d	Progression rate from detected to treatment	0.04
ϕ_d	Hospitalization rate from detected cases	0.03
ϕ_t	Hospitalization rate from treated cases	0.02
μ_t	Mortality rate in treatment class	0.01
θ	Treatment recovery rate	0.06
ξ	Vaccination rate	0.02
η	Loss of vaccine immunity rate	0.01
μ_h	Baseline hospital mortality rate	0.02
$\mu_h\{\max\}$	Maximum hospital mortality rate	0.10
k	Sigmoid steepness parameter	0.5
$Q_{\{\text{crit}\}}$	Critical hospital capacity threshold	50
ρ	Relative infectivity of detected individuals	0.3
κ	Treatment effectiveness scaling factor	5

2.2 Mathematical Analysis of the SUDTHREV Model

We consider the dynamical system defined in (2.1) on the feasible region

$$\Omega = \left\{(S, U, D, T, H, R, E, V) \in \mathbb{R}_+^8 : N(t) \leq N_0\right\}, \tag{2.3}$$

where $N(t) = S + U + D + T + H + R + E + V$ is defined as the total population and N_0 is the initial total population. Standard arguments based on the Lipschitz continuity of the right-hand side ensure existence and uniqueness of solutions.

2.2.1 Positivity and Invariant Region

Theorem 2.1 (Positivity of Solutions)**.** *For non-negative initial conditions, all state variables remain non-negative for all* $t > 0$*.*

Proof. Consider, for instance,

$$\dot{S} = -\beta(1 - w_1)S(U + \rho D) - \xi w_4 S + \eta V.$$

At $S = 0$, we have $\dot{S} = \eta V \geq 0$, hence $S(t) \geq 0$. Similar arguments apply to all compartments, ensuring invariance of $\mathbb{R}^8_+$. □

Theorem 2.2 (Boundedness)**.** *All solutions of system* (2.1) *are uniformly bounded in* Ω.

Proof. Summing all equations gives

$$\frac{dN}{dt} = -\mu_t T - \bar{\mu}_h(Q)H \leq 0,$$

which implies $N(t) \leq N(0)$. Hence, the region Ω is positively invariant. □

2.2.2 Disease-Free Equilibrium and Basic Reproduction Number

The disease-free equilibrium (DFE) is obtained by setting infectious compartments to zero:

$$\mathcal{E}_0 = (S^*, 0, 0, 0, 0, 0, 0, V^*), \tag{2.4}$$

where

$$S^* = \frac{\eta}{\eta + \xi w_4} N_0 \left(1 + \frac{\rho\delta w_2}{\rho_d + \phi_d}\right), \quad V^* = \frac{\xi w_4}{\eta + \xi w_4} N_0. \tag{2.5}$$

To compute the basic reproduction number $\mathcal{R}_0$, we employ the next-generation matrix method. Let

$$\mathcal{F} = \begin{pmatrix} \beta(1-w_1)S(U + \rho D) \\ 0 \\ 0 \\ 0 \end{pmatrix}, \quad \mathcal{V} = \begin{pmatrix} (\gamma + \sigma_u + \delta w_2)U \\ -\delta w_2 U + (\sigma_d + \phi_d)D \\ -\sigma_u U - \sigma_d D + (\phi_t + \mu_t)T \\ -\phi_d D - \phi_t T + (\theta w_3 + \bar{\mu}_h)H \end{pmatrix}. \tag{2.6}$$

The Jacobians evaluated at the DFE yield matrices $\mathcal{F}$ and $\mathcal{V}$, and

$$\mathcal{R}_0 = \rho(FV^{-1}), \tag{2.7}$$

where $\rho(\cdot)$ denotes the spectral radius. After simplification,

$$\mathcal{R}_0 = \frac{\beta(1-w_1)S^*}{\gamma + \sigma_u + \delta w_2}, \tag{2.8}$$

Substituting S^* into (2.8), we have

$$R_0 = \frac{\beta(1-w_1)}{\gamma + \delta w_2 + \sigma_u} \cdot \frac{\eta}{\eta + \xi w_4} N_0 \left(1 + \frac{\rho\delta w_2}{\rho_d + \phi_d}\right). \tag{2.9}$$

The R_0 shows the combined impact of intervention strategies. In particular, transmission control (w_1) directly reduces infection generation, testing (w_2) increases removal from the infectious class, and vaccination (w_4) reduces the susceptible population.

2.2.3 Local Stability of the Disease-Free Equilibrium

Theorem 2.3. *The disease-free equilibrium* $\mathcal{E}_0$ *is locally asymptotically stable if* $\mathcal{R}_0 < 1$ *and unstable if* $\mathcal{R}_0 > 1$.

Proof. The Jacobian matrix evaluated at $\mathcal{E}_0$ has eigenvalues determined by the characteristic equation

$$\det(J - \lambda I) = 0.$$

where

$$J = \begin{pmatrix} \beta(1-w_1)S^* - (\gamma + \sigma_u + \delta w_2) & \beta(1-w_1)\rho S^* \\ \delta w_2 & -(\sigma_d + \phi_d) \end{pmatrix}.$$

The dominant eigenvalue satisfies

$$\lambda = \frac{\text{tr}(J) \pm \sqrt{\text{tr}(J)^2 - 4\det(J)}}{2}.$$

Thus, Re$(\lambda) < 0$ if and only if $\mathcal{R}_0 < 1$, establishing local stability. □

2.2.4 Endemic Equilibrium and Nonlinear Stability

For $\mathcal{R}_0 > 1$, an endemic equilibrium $\mathcal{E}^*$ exists. It satisfies the nonlinear algebraic system:

$$\beta(1 - w_1)S^*(U^* + \rho D^*) = (\gamma + \sigma_u + \delta w_2)U^*, \tag{2.10}$$

with coupled equations for other compartments. The nonlinear hospital mortality term

$$\bar{\mu}_h(H) = \mu_h + \frac{\mu_h^{\max} - \mu_h}{1 + e^{-k(H - Q_{\text{crit}})}} \tag{2.11}$$

introduces state-dependent feedback, making the system non-polynomial.

Theorem 2.4 (Global Stability under Threshold Condition)**.** *If $\mathcal{R}_0 < 1$, the disease-free equilibrium is globally asymptotically stable in Ω.*

Proof. Consider the Lyapunov function

$$\mathcal{L} = U + a_1 D + a_2 T + a_3 H,$$

where $a_i > 0$ are constants to be determined. Differentiating along solutions of the system gives

$$\frac{d\mathcal{L}}{dt} = \dot{U} + a_1 \dot{D} + a_2 \dot{T} + a_3 \dot{H}.$$

Substituting the model equations and grouping terms appropriately, the coefficients a_i can be chosen such that

$$\frac{d\mathcal{L}}{dt} \leq (\mathcal{R}_0 - 1)U.$$

Thus, if $\mathcal{R}_0 < 1$, then $\frac{d\mathcal{L}}{dt} \leq 0$, with equality holding only when $U = D = T = H = 0$. By LaSalle's invariance principle, all trajectories approach the largest invariant set contained in

$$\{(U, D, T, H) : \dot{\mathcal{L}} = 0\},$$

which reduces to the disease-free equilibrium $\mathcal{E}_0$. Therefore, $\mathcal{E}_0$ is globally asymptotically stable. □

2.3 Optimal Control Formulation

Let $x(t) = (S, U, D, T, H, R, E, V)^\top \in \mathbb{R}_+^8$, $w(t) = (w_1, w_2, w_3, w_4)^\top \in \mathcal{U}$, and $\lambda(t) \in \mathbb{R}^8$, where

$$\mathcal{U} = \{w \in L^\infty(0, T)^4 : 0 \leq w_1 \leq 0.8,\ 0 \leq w_j \leq 1,\ j = 2, 3, 4\}. \tag{2.12}$$

The compact form of the controlled SUDTHREV system is as follows:

$$\dot{x}(t) = f(x(t), w(t)), \tag{2.13}$$

where f incorporates the saturation-dependent mortality term defined as

$$\bar{\mu}_h(H) = \mu_h + \frac{\mu_h^{\max} - \mu_h}{1 + e^{-k(H - Q_{\text{crit}})}}. \tag{2.14}$$

The optimal control problem is defined as

$$\min J(w) = \int_0^T \Big[A_1 x_2 + A_2 x_5 + \frac{A_3}{2} x_4^2 + A_4 (x_2 - x_3)^2 + A_5 \bar{\mu}_h(x_5) x_5 + \sum_{i=1}^{4} \frac{B_i}{2} w_i^2\Big] dt + A_6 x_7(T), \quad (2.15)$$

subject to (2.13). Since the integrand is convex in w, and the state system is Lipschitz continuous in x, we have

$$J(w) \geq 0, \quad \forall w \in \mathcal{U}, \quad (2.16)$$

and $\mathcal{U}$ is convex and compact in the weak-* topology of L^∞. The Hamiltonian is given by:

$$\mathcal{H}(x, w, \lambda) = A_1 x_2 + A_2 x_5 + \frac{A_3}{2} x_4^2 + A_4 (x_2 - x_3)^2 + A_5 \bar{\mu}_h(x_5) x_5 + \frac{1}{2} \sum_{i=1}^{4} B_i w_i^2 + \lambda^\top f(x, w). \quad (2.17)$$

The necessary conditions (Pontryagin Maximum Principle) yield

$$\begin{cases} \dot{x}(t) = f(x, w), \\ \dot{\lambda}(t) = -\nabla_x \mathcal{H}(x, w, \lambda), \\ w(t) = \Pi_{\mathcal{U}}\big(- B^{-1} \nabla_w (\lambda^\top f)\big), \end{cases} \quad (2.18)$$

with

$$x(0) = x_0, \quad \lambda(T) = (0, 0, 0, 0, 0, 0, A_6, 0)^\top. \quad (2.19)$$

In particular, the healthcare saturation term contributes nonlinearly:

$$\frac{\partial \mathcal{H}}{\partial x_5} = \cdots - \lambda_5 \bar{\mu}_h(H) + \lambda_7 \bar{\mu}_h(H) - (\lambda_5 - \lambda_7) H \bar{\mu}_h'(H), \quad (2.20)$$

where

$$\bar{\mu}_h'(H) = \frac{k(\mu_h^{\max} - \mu_h) e^{-k(H - Q_{\text{crit}})}}{(1 + e^{-k(H - Q_{\text{crit}})})^2}.$$

and the adjoint equation for H becomes

$$\dot{\lambda}_5 = -A_2 - A_5(\bar{\mu}_h + x_5 \bar{\mu}_h') + (\theta w_3 + \bar{\mu}_h)\lambda_5 - \theta w_3 \lambda_6 - \bar{\mu}_h \lambda_7 + (\lambda_5 - \lambda_7) x_5 \bar{\mu}_h'. \quad (2.21)$$

The optimal controls satisfy

$$\frac{\partial \mathcal{H}}{\partial w_i} = 0, \quad i = 1, \ldots, 4, \quad (2.22)$$

the general form gives

$$\tilde{w}_i(t) = -\frac{1}{B_i} \frac{\partial}{\partial w_i} \big(\lambda^\top f(x, w)\big), \quad (2.23)$$

and the admissible optimal controls are

$$w_i^*(t) = \Pi_{[0, w_i^{\max}]} \left(\tilde{w}_i(t)\right), \quad (2.24)$$

yielding

$$\begin{aligned} w_1^* &= \Pi\left(\frac{\beta x_1 x_2 (\lambda_2 - \lambda_1)}{B_1}\right) \\ w_2^* &= \Pi\left(\frac{\delta x_2 (\lambda_2 - \lambda_3)}{B_2}\right) \\ w_3^* &= \Pi\left(\frac{\theta x_5 (\lambda_5 - \lambda_6)}{B_3}\right) \\ w_4^* &= \Pi\left(\frac{\xi x_1 (\lambda_1 - \lambda_8)}{B_4}\right) \end{aligned} \quad (2.25)$$

where Π denotes projection. The operator $\Pi_{[0,w_i^{\max}]}$ denotes the orthogonal projection onto the admissible control set $[0, w_i^{\max}]$, ensuring that the optimal controls satisfy the imposed bounds. Thus,

$$\frac{\partial w_3^*}{\partial x_5} \propto (\lambda_5 - \lambda_6)\left(1 + x_5 \bar{\mu}_h'\right), \tag{2.26}$$

showing explicit dependence of optimal control on saturation.

2.3.1 Forward Backward Sweep Operator

We define the operator

$$\mathcal{T} : w^{(k)} \mapsto w^{(k+1)} \tag{2.27}$$

through the iterative process described below, which is Forward Sweep, Backward Sweep, and Control Update, respectively:

$$\dot{x}^{(k)} = f(x^{(k)}, w^{(k)}), \quad x^{(k)}(0) = x_0, \tag{2.28}$$

$$\dot{\lambda}^{(k)} = -\nabla_x \mathcal{H}(x^{(k)}, w^{(k)}, \lambda^{(k)}), \quad \lambda^{(k)}(T) = \lambda_T, \tag{2.29}$$

$$w^{(k+1)} = \Pi_{\mathcal{U}}\left(-B^{-1}\nabla_w(\lambda^{(k)\top} f(x^{(k)}, w^{(k)}))\right). \tag{2.30}$$

Let $0 = t_0 < t_1 < \cdots < t_N = T$, with step size $h = \frac{T}{N}$. The fourth order RungeKutta) is given as:

$$x_{n+1}^{(k)} = x_n^{(k)} + \frac{h}{6}(k_1 + 2k_2 + 2k_3 + k_4), \tag{2.31}$$

where

$$k_1 = f(x_n^{(k)}, w_n^{(k)}), \quad k_2 = f(x_n^{(k)} + \tfrac{h}{2}k_1, w_n^{(k)}),$$
$$k_3 = f(x_n^{(k)} + \tfrac{h}{2}k_2, w_n^{(k)}), \quad k_4 = f(x_n^{(k)} + hk_3, w_n^{(k)}).$$

and backward integration

$$\lambda_n^{(k)} = \lambda_{n+1}^{(k)} - \frac{h}{6}(\ell_1 + 2\ell_2 + 2\ell_3 + \ell_4), \tag{2.32}$$
$$\ell_1 = \nabla_x \mathcal{H}(x_{n+1}^{(k)}, w_{n+1}^{(k)}, \lambda_{n+1}^{(k)}),$$

and similarly for ℓ_2, ℓ_3, ℓ_4. While the control update is provided as:

$$w_{i,n}^{(k+1)} = \Pi_{[0,w_i^{\max}]}\left(-\frac{1}{b_i}\frac{\partial}{\partial w_i}\left(\lambda_n^{(k)\top} f(x_n^{(k)}, w_n^{(k)})\right)\right). \tag{2.33}$$

2.3.2 Convergence Analysis

We define the norm

$$\|w\|_\infty = \sup_{t\in[0,T]} |w(t)|. \tag{2.34}$$

and assume

$$\|f(x_1, w_1) - f(x_2, w_2)\| \le L(\|x_1 - x_2\| + \|w_1 - w_2\|), \tag{2.35}$$

where $f(x, w)$ is Lipschitz in x and w, $\nabla_x \mathcal{H}$ is Lipschitz, and $\bar{\mu}_h(H) \in C^1$ with bounded derivative with

$$L = L_0 + C\bar{\mu}_h'(H). \tag{2.36}$$

Then

$$\|x^{(k)} - x^{(k-1)}\|_\infty \le LT\|w^{(k)} - w^{(k-1)}\|_\infty, \tag{2.37}$$
$$\|\lambda^{(k)} - \lambda^{(k-1)}\|_\infty \le LT\|x^{(k)} - x^{(k-1)}\|_\infty. \tag{2.38}$$

Hence,

$$\|w^{(k+1)} - w^{(k)}\|_\infty \le CL^2T^2\|w^{(k)} - w^{(k-1)}\|_\infty. \tag{2.39}$$

Theorem 2.5 (Convergence)**.** *If*

$$CL^2T^2 < 1, \tag{2.40}$$

then $\mathcal{T}$ is a contraction and $w^{(k)} \to w^*$.

Proof. From (2.28)(2.30), we obtain

$$\|x^{(k)} - x^{(k-1)}\|_\infty \leq LT\|w^{(k)} - w^{(k-1)}\|_\infty,$$

$$\|\lambda^{(k)} - \lambda^{(k-1)}\|_\infty \leq LT\|x^{(k)} - x^{(k-1)}\|_\infty.$$

Thus,

$$\|w^{(k+1)} - w^{(k)}\|_\infty \leq CL^2T^2\|w^{(k)} - w^{(k-1)}\|_\infty.$$

If $CL^2T^2 < 1$, then $\mathcal{T}$ is a contraction. □

3 Results and Discussion

Simulations were performed over a time horizon of 100 units with a population of 10^6, initialized according to Table 3. In Fig. 1, the uncontrolled scenario shows a quick rise in unreported infections U, peaking at roughly 3.2×10^5, followed by a delayed hospitalisation peak near 2.5×10^4. The optimal control strategy decreases infection peak to 5.0×10^4 and hospitalisation to 1.0×10^4, with both curves showing monotonic decay rather than explosive rise. The system experiences a regime transition

Table 3: Simulation Setup

Quantity	Value
Total population N_0	1,000,000
Simulation time	100 units
Time steps	500
Initial susceptible	90%
Initial infected U	5%
Initial detected D	2%
Initial treated T	1%
Initial hospitalized H	1%
Initial vaccinated V	1%

under optimal control, as indicated by this stark contrast. The uncontrolled dynamics depict an epidemic spike caused by nonlinear transmission, whereas the controlled system enters a subcritical state in which infections decrease promptly after commencement. Early and sustained activation of transmission control w_1 significantly decreases the force of infection $\beta(1 - w_1)SU$. This prevents the system from entering the nonlinear amplification phase, which is often linked with epidemic peaks as it was shown in Fig 1. This result corroborates with the recent studies on epidemic management that demonstrate that early intervention predominates over late-stage mitigation (e.g., optimal control assessments in COVID-19 and Ebola models) (Aldila et al., 2022; Mondal and Khajanchi, 2022; Keita et al., 2023; Xia et al., 2024). Studies that emphasise time-dependent control over static interventions have revealed similar peak suppression patterns (Bolzoni et al., 2017; Zhang et al., 2021; Bulai et al., 2023; Olaiju et al., 2025a).

Figure 2 illustrates how, under optimal control, mortality is significantly decreased and shows a gradual, near-linear accumulation, whereas in the uncontrolled situation, cumulative fatalities rise dramatically. Over time, the two curves' divergence gets wider. The model's nonlinear mortality

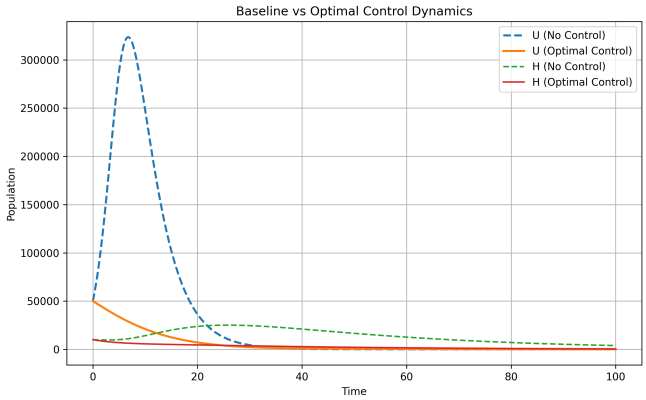

Figure 1: Epidemic dynamics: baseline versus optimal control. Time evolution of unreported infections (U) and hospitalisations (H) for uncontrolled and optimally regulated scenarios.

amplification mechanism is reflected in this pattern through: $\bar{\mu}_h(H)$. This was demonstrated in Figure 2, which illustrates how healthcare saturation causes mortality to climb nonlinearly as hospitalisations rise. Optimal control, on the other hand, keeps the system out of this high-mortality regime by decreasing hospital load (H) through both treatment improvement and transmission reduction. This is consistent with Boyer et al. (2024) recent discoveries in epidemiological modelling, which show that limitations in healthcare capacity serve as tipping points for increases in mortality. Studies that take saturation effects into account repeatedly show that hospitalisation control, as opposed to infection control alone, is highly sensitive to mortality reduction (Steier and Moxham, 2020; Stachel et al., 2021).

In the uncontrolled situation, daily deaths peak above 3,500 instances, but with optimal control, the peak stays below 400, as seen in Figure 3. Furthermore, the regulated curve is flattened and stretched, whereas the uncontrolled curve has a prominent bell-shaped apex. This is a direct result of lowering the rate at which people enter severe categories, as shown by the flattening of the death curve in Figure 3. Acute spikes linked to healthcare overload are avoided by the controlled system, which spreads death over time. Although flattening the curve lowers peak mortality without necessarily eliminating cumulative deaths completely, this behaviour is consistent with widely reported results in epidemic modelling literature (Kantner and Koprucki, 2020; Zizler and Sobhanzadeh, 2021; Mondal and Khajanchi, 2022; Ahmed et al., 2022). However, Figure 3 goes beyond this by demonstrating simultaneous reduction in both peak and cumulative deaths due to nonlinear mortality control.

Cumulative deaths consistently decrease as (κ) increases. As observed in Figure 4, higher values of (κ) flatten the mortality curve and reduce its asymptotic level. The hospitalised compartment's recovery and survival rates are directly impacted by the parameter (κ). Its effect is both nonlinear and monotonic, suggesting that mortality decreases as treatment efficacy increases. Crucially, this parameter does not considerably change infection trajectories, indicating a disconnection between clinical consequences and transmission patterns. This result is consistent with research by Raus et al. (2022); Lawrence (2024); Abiri et al. (2025) and Björk et al. (2026) that distinguishes between pharmaceutical (treatment) and non-pharmaceutical (transmission) interventions, where therapy increases survival but has no effect on disease spread. Additionally, Figure 4 supports the findings of Akinsunmade

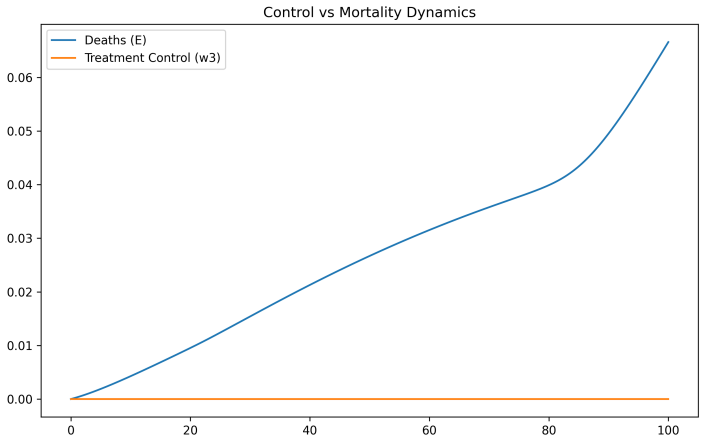

Figure 2: Cumulative mortality under control and no-control scenarios. Comparison of cumulative deaths (E) with and without optimal control.

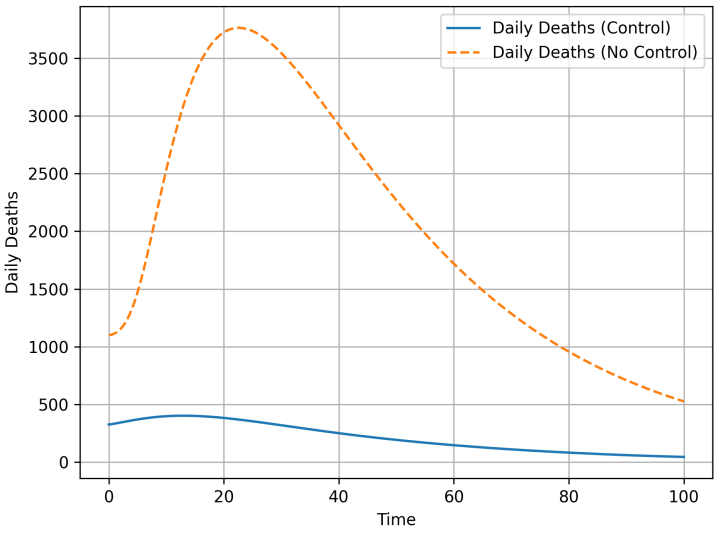

Figure 3: Daily mortality dynamics and curve flattening. Daily fatalities under baseline and optimal control conditions.

and Afolabi (2026) that treatment effectiveness is a mortality control lever rather than a transmission control mechanism, highlighting the necessity of coordinated intervention strategies.

Figure 5 shows that the temporal behaviours of the controls differ: w_1 is consistently high; w_2 is low and delayed; w_3 is growing mid-epidemic; and w_4 is non-monotonic. It suggests a multi-phase control strategy in which treatment and selective vaccine changes are employed to accomplish

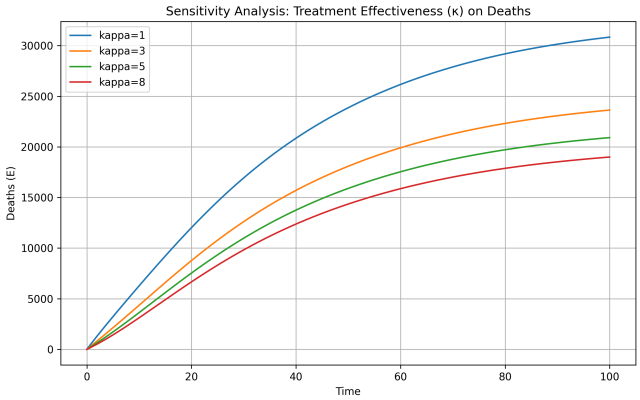

Figure 4: Sensitivity analysis of the mortality impact of treatment effectiveness (κ). effects of different treatment efficacy on total fatalities.

mid-phase stability and early suppression through transmission control. Under robust transmission control, testing w_2 has a relatively tiny contribution, indicating a minimal marginal gain. This is consistent with optimum control studies that demonstrate that control prioritisation naturally arises from system dynamics and that not all actions contribute equally (Olaiya et al., 2019; Kuddus et al., 2024; Zhu et al., 2025). As demonstrated in Figure 5, uniform intervention tactics are invalidated because optimal policies are intrinsically heterogeneous and time-dependent.

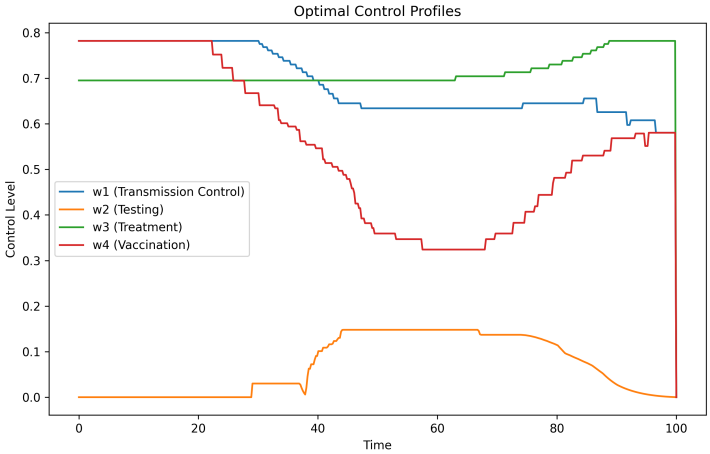

Figure 5: Time-dependent control profiles that are optimal. Over the course of the simulation, the best intervention options for immunisation (w_4), testing (w_2), treatment (w_3), and transmission reduction (w_1).

Figure 6 illustrates how the reproduction number falls linearly with (w_1), reaching the crucial

barrier $(R_0 = 1)$ at roughly $(w_1 \approx 0.7)$. Sustained transmission is prevented by keeping (w_1) above this threshold, which guarantees the system stays in a subcritical state. The findings demonstrate that the model has operational relevance by directly connecting this threshold to ideal control trajectories.

Table 4: Policy comparison between baseline and optimal control scenarios.

Scenario	**Peak U**	**Deaths**	**Death Reduction (%)**	**Cost**	**ICER**
Baseline	323,504.81	204,553.10	0.00	0.00	–
Optimal Control	50,000.00	21,384.26	89.55	67.91	2.20×10^{-5}

Table 4 reveals that the baseline scenario shows a peak hospitalisation of 2.51×10^4, a peak infection of 3.24×10^5, and a cumulative death toll of 2.05×10^5. These values significantly decrease to 5.0×10^4, 1.0×10^4, and 2.14×10^4 under optimal control. At a total intervention cost of roughly 67.91, this translates to a 84.99% decrease in infections and a 89.55% decrease in deaths, with an ICER of about 10^{-5}. The optimal control strategy functions across epidemiological pathways, as evidenced by the simultaneous decrease in infection load and mortality Olaiju et al. (2025b). Transmission control (w_1), which lowers the force of infection, is the main factor contributing to the decrease in peak infection. However, the greater decrease in mortality suggests that intervention control (w_3), which slows the path to fatal outcomes, may also have contributed. Controlling hospitalisation avoids entry into high-fatality regimes, which is why the difference between infection reduction $\approx 85\%$ and death reduction $\approx 90\%$ demonstrates the impact of the nonlinear mortality function. The system functions in a high-efficiency regime, where minor increases in control cost result in disproportionately huge reductions in disease burden, as further demonstrated by the low ICER.

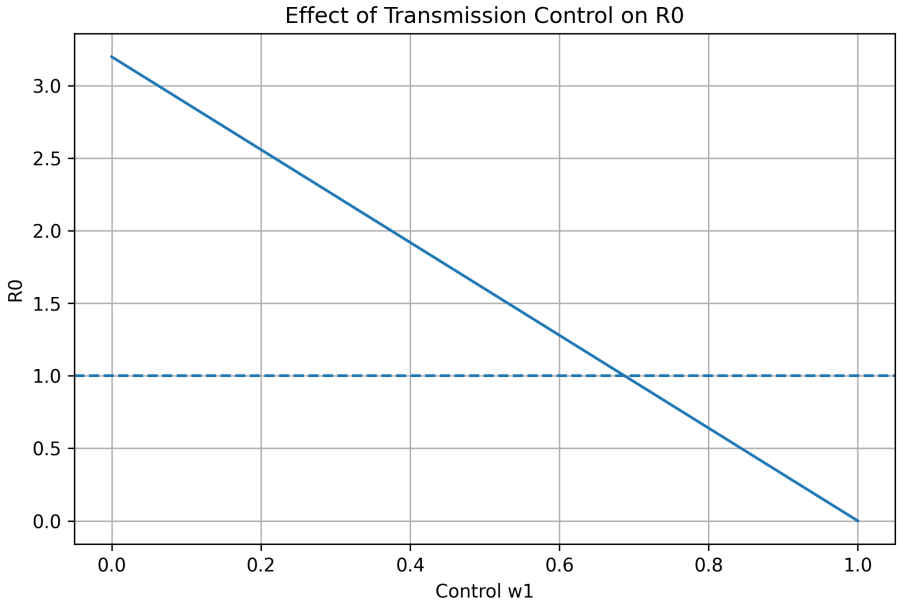

Figure 6: The basic reproduction number is affected by transmission control. The effective reproduction number (R_0) and transmission control intensity (w_1) are related.

Furthermore, models that incorporate nonlinear hospital saturation effects (Boyer et al., 2024) show that averting capacity exceedance results in significant survival gains, which is consistent with the observed amplification in mortality reduction relative to infection reduction. Crucially, the high cost-effectiveness shows that time-dependent, well-structured treatments can have a significant epidemiological impact without requiring excessive resource outlay, supporting their viability in practical contexts.

4 Conclusion

In this study, a nonlinear optimal control framework for an SUDTHREV epidemiological framework that considers transmission dynamics, staged disease progression, and mortality dependent on healthcare capacity was developed. A key component of the model is the sigmoidal hospital-induced mortality function, which shows the transition from baseline fatality to saturation-driven escalation as hospitalisation exceeds a critical threshold.

By applying the Pontryagin Maximum Principle for the solution of the optimal control problem, a coupled forward-backward system is obtained. The numerical simulations of the problem revealed that the intervention strategies are not only time-dependent but also phase-dependent. The controlled system immediately reaches a stable decay regime, whereas the uncontrolled system follows classical nonlinear outbreak dynamics with fast infection growth and delayed peaks in hospitalization. In addition to this significant structural change in the dynamics of the epidemiological outbreak, considerable reductions in the epidemiological burden are also obtained, including a 90% reduction in cumulative deaths and an 85% reduction in peak infections, all of which are obtained for relatively low intervention

costs.

The findings suggest that efficient management of epidemics is, in essence, a nonlinear system regulation problem with resource constraints, and early, sustained, and adaptive interventions can significantly alleviate the burden of infections and mortality with minimal associated costs, which has significant implications for public health policy. Further studies in this direction are needed to incorporate data-based calibration, stochastic effects, and uncertainties in parameters, which will allow for real-time optimization in dynamic epidemic scenarios.

References

Abiri, E., Raesi, R., and Kashani, M. H. G. (2025). The role and position of non-pharmacological interventions (NPI) in the management and control of emerging and re-emerging infectious diseases in the post-COVID-19 era: A systematic review. *The Open Public Health Journal*, 18(1):e18749445367433.

Ahmed, S., Shemanto, M., Azhari, H., and Zakaria, G. (2022). Estimation of the doubling time and reproduction number for COVID-19. *Computer Methods in Biomechanics and Biomedical Engineering*, 25(6):668–674.

Akinsunmade, A. E. and Afolabi, A. O. (2026). Mathematical model for trypanosomiasis management integrating treatment enhancement, vector control, and host management strategies. *Frontiers in Applied Mathematics and Statistics*, 12:100500.

Aldila, D., Shahzad, M., Khoshnaw, S. H., Ali, M., Sultan, F., Islamilova, A., Anwar, Y. R., and Samiadji, B. M. (2022). Optimal control problem arising from covid-19 transmission model with rapid-test. *Results in Physics*, 37:105501.

Antony Oliver, M. C., Graham, M., Manolopoulou, I., Medley, G. F., Pellis, L., Pouwels, K. B., Thorpe, M., and Hollingsworth, T. D. (2025). Uncertainty quantification in cost-effectiveness analysis for stochastic-based infectious disease models: Insights from surveillance on lymphatic filariasis. *Journal of Theoretical Biology*, 611:112197.

Biswas, S., Subramanian, A., ELMojtaba, I. M., Chattopadhyay, J., and Sarkar, R. R. (2017). Optimal combinations of control strategies and cost-effective analysis for visceral leishmaniasis disease transmission. *PLOS ONE*, 12(2):e0172465.

Björk, J., Rasmussen, G., Johansson, S., Dagerhamn, J., Olofsson, H., and Ramsay, K. W. (2026). Non-pharmaceutical interventions to prevent community transmission of infectious diseases with pandemic potential—an umbrella review and evidence map. *European Journal of Public Health*, 36(1):200–207.

Bolzoni, L., Bonacini, E., Soresina, C., and Groppi, M. (2017). Time-optimal control strategies in SIR epidemic models. *Mathematical Biosciences*, 292:86–96. Epub 2017 Aug 8.

Boyer, L., Pauly, V., Brousse, Y., et al. (2024). The impact of hospital saturation on non-COVID-19 hospital mortality during the pandemic in France: a national population-based cohort study. *BMC Public Health*, 24(1):1798.

Bulai, I. M., Montefusco, F., and Pedersen, M. G. (2023). Stability analysis of a model of epidemic dynamics with nonlinear feedback producing recurrent infection waves. *Applied Mathematics Letters*, 136:108455.

Caravaggio, A., Di Liddo, A., and Martiradonna, A. (2026). When cures are costly: Budget-constrained epidemic control and strategic drug pricing. *Journal of Economic Behavior & Organization*, 245:107529.

Durojaye, M. O. and Odeyemi, J. K. (2019). Radial basis function-finite difference (RBF-FD) approximations for two-dimensional heat equations. *The Pacific Journal of Science and Technology*, 20(2):43–49.

Durojaye, M. O., Odeyemi, J. K., and Ajie, I. J. (2019). Numerical solution of two dimensional Laplace's equation on a regular domain using Chebyshev differentiation matrices. *Physical Science International Journal*, 23(1):1–7.

Falodun, M. O., Olorunfemi, O., and Irinoye, O. O. (2025). Infectious diseases: Addressing global challenges and prevention strategies for national health improvement. *Community Acquired Infection*, 12:e0533.

Grassly, N. C. and Fraser, C. (2008). Mathematical models of infectious disease transmission. *Nature Reviews Microbiology*, 6(6):477–487.

Hakim, S. and Haque, M. A. (2026). Health system capacity for infectious disease pandemic response in low- and lower-middle-income countries: Insights from national health facility surveys. *International Journal of Infectious Diseases*, 163:108281.

Idisi, O. I., Yusuf, T. T., Owolabi, K. M., and Oshinubi, K. (2025). Optimal control strategies for Dual-Strain SARS-CoV-2 dynamics with Cost-Effectiveness analysis. *Computation*, 13(6):135.

Kaba, M., Abunna, F., Tiku Mereta, S., Kitaw, Y., and Abdissa, A. (2025). Containing emerging and re-emerging infections: A continuing global health challenge. In IntechOpen, editor, *Public Health*. IntechOpen, London, UK. Chapter available from IntechOpen Open Access.

Kantner, M. and Koprucki, T. (2020). Beyond just "flattening the curve": Optimal control of epidemics with purely non-pharmaceutical interventions. *Journal of Mathematics in Industry*, 10(1):23.

Keita, M., Talisuna, A., Chamla, D., Burmen, B., Cherif, M. S., Polonsky, J. A., et al. (2023). Investing in preparedness for rapid detection and control of epidemics: analysis of health system reforms and their effect on 2021 ebola virus disease epidemic response in Guinea. *BMJ Global Health*, 8(1):e010984.

Khan, A. A., Ullah, S., and Amin, R. (2022). Optimal control analysis of COVID-19 vaccine epidemic model: A case study. *The European Physical Journal Plus*, 137(1):156. Erratum in: Eur Phys J Plus. 2022;137(2):198.

Kowalewska, A., Krawczyk, J., Bodnar, M., and Vela-Pérez, M. (2026). Exploring the impact of healthcare capacity and time delays in SIR epidemic model. *Mathematics and Computers in Simulation*, 241:771–782.

Kretzschmar, M. and Wallinga, J. (2009). Mathematical models in infectious disease epidemiology. In Krämer, A., Kretzschmar, M., and Krickeberg, K., editors, *Modern Infectious Disease Epidemiology*, pages 209–221. Springer, New York, NY.

Kretzschmar, M. E., Ashby, B., Fearon, E., Overton, C. E., Panovska-Griffiths, J., Pellis, L., Quaife, M., Rozhnova, G., Scarabel, F., Stage, H. B., Swallow, B., Thompson, R. N., Tildesley, M. J., and Villela, D. (2022). Challenges for modelling interventions for future pandemics. *Epidemics*, 38:100546.

Kuddus, M., Paul, A. K., and Theparod, T. (2024). Cost-effectiveness analysis of COVID-19 intervention policies using a mathematical model: An optimal control approach. *Scientific Reports*, 14(1):494.

Lawrence, A. (2024). Evaluating the effectiveness of public health measures during infectious disease outbreaks: A systematic review. *Cureus*, 16(3):e55893.

Liu, W., Zou, G., Bao, Q., and Wang, S. (2025). Optimal prevention and control strategy of infectious disease: Cost-effectiveness analysis based on a modified dynamic model with economic loss. *Infectious Disease Modelling*, 11(1):377–388.

Madhav, N., Oppenheim, B., Gallivan, M., Mulembakani, P., Rubin, E., and Wolfe, N. (2017). Pandemics: Risks, Impacts, and Mitigation. In Jamison, D. T., Gelband, H., Horton, S., et al., editors, *Disease Control Priorities: Improving Health and Reducing Poverty*, chapter 17. The International Bank for Reconstruction and Development / The World Bank, Washington (DC), 3rd edition. Published 2017 Nov 27.

Marshall, D. A., Burgos-Liz, L., IJzerman, M. J., Osgood, N. D., Padula, W. V., Higashi, M. K., Wong, P. K., Pasupathy, K. S., and Crown, W. (2015). Applying dynamic simulation modeling methods in health care delivery research—the SIMULATE checklist: Report of the ISPOR simulation modeling emerging good practices task force. *Value in Health*, 18(1):5–16.

Martin, C., McDonald, S., Bale, S., Luteijn, M., and Sarkar, R. (2021). Construction of a demand and capacity model for intensive care and hospital ward beds, and mortality from COVID-19. *BMC Medical Informatics and Decision Making*, 21(1):138.

Mondal, J. and Khajanchi, S. (2022). Mathematical modeling and optimal intervention strategies of the covid-19 outbreak. *Nonlinear Dynamics*, 109(1):177–202. Epub 2022 Jan 30.

Nainggolan, J., Ansori, M. F., and Tasman, H. (2025). An optimal control model with sensitivity analysis for COVID-19 transmission using logistic recruitment rate. *Healthcare Analytics*, 7:100375.

Odeyemi, J. K., Olaiya, O. O., and Ogunfiditimi, F. O. (2023). Hermite polynomial-based methods for optimal order approximation of first-order ordinary differential equations. *Journal of Advances in Mathematics and Computer Science*, 38(6):16–32.

Okafor, F. M., Durojaye, M. O., Odeyemi, J. K., and Ogunware, B. G. (2025). A COMPARATIVE STUDY OF STENCIL-BASED METHOD OF LINES FOR SOLVING THE BURGERS-HUXLEY EQUATION. *FUDMA Journal of Sciences*, 9(7):1–7.

Okeke, E. S., Olovo, C. V., Nkwoemeka, N. E., Okoye, C. O., Nwankwo, C. E. I., and Onu, C. J. (2022). Microbial ecology and evolution is key to pandemics: Using the coronavirus model to mitigate future public health challenges. *Heliyon*, 8(5):e09449.

Olaiju, O. A., Akinde, M., Olapeju, O., and Odeyemi, J. K. (2025a). Mathematical modelling of cholera transmission incorporating open defecation as an environmental driver: An optimal control approach. *International Journal of Applied Mathematics*, 38(1s):997–1020.

Olaiju, O. A., Odeyemi, J. K., Akinde, M., Olapeju, O., and Okafor, F. M. (2025b). Mathematical modelling of microbial-nutrient kinetics in biochar amended soils using backward differentiation formula. *Communications in Mathematical Biology and Neuroscience*, 2025:Article–ID.

Olaiya, O. O., Oduwole, H. K., and Odeyemi, J. K. (2019). Numerical solution of Black–Scholes partial differential equation using direct solution of second-order ordinary differential equation with two-step hybrid block method of order seven. *Science World Journal*, 14(2):23–29.

Omosigho, P. O., Okesanya, O. J., Olaleke, N. O., Eshun, G., and Lucero-Prisno, III, D. E. (2023). Multiple burden of infectious disease outbreaks: Implications for Africa healthcare system. *Journal of Taibah University Medical Sciences*, 18(6):1446–1448. Letter to the Editor.

Pathak, S. and Kota, V. R. (2025). Mathematical analysis of an infectious disease model: Stability, Persistence, and Equilibrium analysis in a non-linear epidemiological system. *Journal of Nonlinear Mathematical Physics*, 32(1):64.

Petanidis, S., Chandramouli, K., Floros, G., Nifakos, S., Kolomvatsos, K., Tsekeridou, S., Magalini, S., Gui, D., and Kosmidis, C. (2025). Optimizing emergency response in hospitals: A systematic review of surge capacity planning and crisis resource management. *Healthcare*, 13(21):2819.

Qu, Z., McMahon, B. H., Perkins, D. J., and Hyman, J. M. (2021). Staged progression epidemic models for the transmission of invasive nontyphoidal Salmonella (iNTS) with treatment. *Mathematical Biosciences and Engineering*, 18(2):1529–1549.

Raus, K., Mortier, E., and Eeckloo, K. (2022). Ethical reflections on Covid-19 vaccines. *Acta Clinica Belgica*, 77(3):600–605.

Sanz-Lorenzo, L. and Bravo de la Parra, R. (2024). Discrete-time staged progression epidemic models. *Mathematical and Computer Modelling of Dynamical Systems*, 30(1):496–522.

Shahverdi, B., Miller-Hooks, E., Tariverdi, M., Ghayoomi, H., Prentiss, D., and Kirsch, T. D. (2023). Models for assessing strategies for improving hospital capacity for handling patients during a pandemic. *Disaster Medicine and Public Health Preparedness*, 17:e110.

Shretta, R., Liu, J., Cotter, C., Flower, J., and Schapira, A. (2017). Malaria elimination and eradication. In Holmes, K. K., Bertozzi, S., Bloom, B. R., et al., editors, *Major Infectious Diseases*, chapter 12. The International Bank for Reconstruction and Development / The World Bank, Washington (DC), 3rd edition. Published 2017 Nov 3.

Singla, S. (2020). Demand and capacity modelling in healthcare using Discrete Event Simulation. *Open Journal of Modelling and Simulation*, 8(4):88–107.

Stachel, A., Keegan, L. T., Blumberg, S., and CDC MInD Healthcare Program (2021). Modeling transmission of pathogens in healthcare settings. *Current Opinion in Infectious Diseases*, 34(4):333–338.

Steier, J. and Moxham, J. (2020). The load and capacity model of healthcare delivery: considerations for the crisis management of the COVID-19 pandemic. *Journal of Thoracic Disease*, 12(8):3930–3933. Editorial.

Thokala, P., Duarte, H., Wright, S., Husereau, D., Durand-Zaleski, I., Lindgren, P., Postema, R., Machnicki, G., and Garrison, L. (2025). Incorporating resource constraints in health economic evaluations: Overview and methodological considerations. *PharmacoEconomics - Open*, 9(2):161–178.

Tolles, J. and Luong, T. (2020). Modeling epidemics with compartmental models. *JAMA*, 323(24):2515–2516.

Vugrin, E. D., Verzi, S. J., Finley, P. D., Turnquist, M. A., Griffin, A. R., Ricci, K. A., and Wyte-Lake, T. (2015). Modeling hospitals' adaptive capacity during a loss of infrastructure services. *Journal of Healthcare Engineering*, 6(1):85–120.

Xia, F., Xiao, Y., and Ma, J. (2024). The optimal Spatially-Dependent control measures to effectively and economically eliminate emerging infectious diseases. *PLOS Computational Biology*, 20(10):e1012498.

Xue, L., Huo, J., and Zhang, Y. (2025). Modelling and analysis of an epidemic model with awareness caused by deaths due to fear. *Journal of Biological Dynamics*, 19(1):2458890.

Yadav, S. K. and Akhter, Y. (2021). Statistical modeling for the prediction of infectious disease dissemination with special reference to COVID-19 spread. *Frontiers in Public Health*, 9:645405.

Zhang, L., Ullah, S., Alwan, B. A., Alshehri, A., and Sumelka, W. (2021). Mathematical assessment of constant and time-dependent control measures on the dynamics of the novel coronavirus: An application of optimal control theory. *Results in Physics*, 31:104971. Epub 2021 Nov 12.

Zhu, H., Zheng, J., Huang, J., Zhang, M., Zhou, C., Zhu, T., Tian, H., Wu, X., Liu, Y., Zhong, B., Xie, H., Zhang, L., Tie, L., Luo, J., Mao, X., Zhang, B., Deng, X., Zhang, S., Qian, M., Li, S., and Zhou, X. (2025). Optimal control strategies supported by system dynamics modelling: a study on hookworm disease in China. *Infectious Diseases of Poverty*, 14(1):22.

Zizler, P. and Sobhanzadeh, M. (2021). Flattening the curve. *The Mathematics Enthusiast*, 18(1):Article 20.